Electronic Supplementary Material (ESI) for RSC Advances.

Supporting Information

A Novel Oxaphenalenone, Penicimutalidine: Activated Production of Oxaphenalenones by the Diethyl Sulphate Mutagenesis of Marine-derived Fungus *Penicillium purpurogenum* G59

Chang-Wei Li,[a,‡] Ming-Wen Xia,[a,‡] Cheng-Bin Cui,[a,*] Ji-Xing Peng[b] and De-Hai Li[b]

[a.] *State Key Laboratory of Toxicology and Medical Countermeasures, Beijing Institute of Pharmacology and Toxicology, Beijing 100850, China*

[b.] *Key Laboratory of Marine Drugs, Chinese Ministry of Education, School of Medicine and Pharmacy, Ocean University of China, Qingdao 266003, China*

‡ These authors contributed equally to this work.

* To whom correspondence should be addressed. Email: cuicb@126.com or cuicb@sohu.com; Fax & Tel: 86-10-68211656.

Table of Contents

No.	Content	Page
1	Experimental section.	S3
2	Physicochemical and spectroscopic data of penicimutalidine (**1**).	S7
3	Physicochemical and spectroscopic data of compounds **2–4**.	S8
4	**Figure S1.** DFT-optimized structures for the low-energy conformers of **1** and ***ent*-1** at the B3LYP/6-31+G(d) level using a polarizable continuum model (PCM) in MeOH.	S9
5	**Figure S2.** DFT-optimized structures for the low-energy conformers of **4** and ***ent*-4** at the B3LYP/6-31+G(d) level using a polarizable continuum model (PCM) in MeOH.	S9
6	**Figure S3.** HPLC-ESI-MS analysis of the EtOAc extracts of the mutant AD-1-1 and parent G59 strains to detect **1–4**.	S10
7	**Figure S4.** HPLC-PDAD-UV analysis of the EtOAc extracts of the mutant AD-1-1 and parent G59 strains to detect **1–4**.	S12
8	**Figure S5.** Positive and negative ESIMS spectra of **1.**	S13
9	**Figure S6.** Positive HRESIMS spectrum of **1.**	S13
10	**Figure S7.** UV spectrum of **1** in MeOH.	S13
11	**Figure S8.** IR spectrum of **1** (measured on an ATR crystal).	S14
12	**Figure S9.** 400 MHz ^{1}H NMR spectrum of **1** in acetone-d_6.	S14
13	**Figure S10.** 100 MHz ^{13}C NMR spectrum of **1** in acetone-d_6.	S15
14	**Figure S11.** 400 MHz ^{1}H-^{1}H COSY spectrum of **1** in acetone-d_6.	S15
15	**Figure S12.** 400 MHz ^{1}H/100 MHz ^{13}C HMQC spectrum of **1** in acetone-d_6.	S16
16	**Figure S13.** 400 MHz ^{1}H/100 MHz ^{13}C HMBC spectrum of **1** in acetone-d_6.	S16
17	**Figure S14**. 400 MHz ^{1}H NMR spectrum of **4** in acetone-d_6.	S17
18	**Figure S15**. 100 MHz ^{13}C NMR spectrum of **4** in acetone-d_6.	S17

Experimental Section

General Experimental Procedures. Melting points were measured on a Beijing Tiandiyu X-4 exact micro melting point apparatus (Tiandiyu science and technology Co., Ltd, Beijing, China) and the temperatures were not corrected. Optical rotations were recorded on an Optical Activity Limited PolAAr 3005 spectropolarimeter (Optical Activity Limited, Ramsey, UK). ESIMS and HRESIMS were measured on an AB SCIEX Applied Biosystems API 3000 LC-MS (AB SCIEX, Framingham, MA, USA) and an Agilent 6520 Q-TOF LC-MS (Agilent Technologies, Santa Clara, CA, USA) spectrometers, respectively. UV data were acquired with a Varian CARY300 spectrophotometer (Varian, Palo Alto, USA). IR spectra were recorded on a Bruker Tensor-27 infrared spectrophotometer (Bruker, Karlsruhe, Germany). CD data were measured on a Bio-Logic Science MOS450 CD spectrometer (Bio-Logic, Pont-de-Claix, France). NMR spectra were acquired on a JEOL JNM-GX 400 (400 MHz for ^{1}H/100 MHz for ^{13}C) NMR spectrometer (JEOL Ltd, Tokyo, Japan). TLC was performed using pre-coated silica gel GF_{254} plates (0.25-mm thickness, Yantai Chemical Industrial Institute, Yantai, China), and the TLC spots were detected under sunlight/UV light (254 and 365 nm) illumination or using Vaughan's reagent.[1] Column chromatography was performed using Silica gel H (200–300 mesh, Yantai Chemical Industrial Institute, Yantai, China). HPLC was performed on a Waters HPLC system equipped with a Waters 600 controller, a Waters 600 pump, a Waters 2414 refractive index detector, and a Waters 2996 (for analytical HPLC) or 2998 (for preparative HPLC) photodiode array detector using Waters Empower™ software (Waters, Milford, MA, USA). Venusil MP C_{18} (5 μm, 100 Å, 4.6 × 250 mm; Agela Technologies, Tianjin, China) and Capcell Pak C_{18} (MG II, 4.6 × 250 mm; Shiseido Co., Ltd, Tokyo, Japan) columns were used for analytical HPLC and a Capcell Pak C_{18} (MG II, 20 × 250 mm; Shiseido Co., Ltd, Tokyo, Japan) column was used for preparative HPLC. Cell morphology was examined using an AE31 EF-INV inverted microscope (Motic China Group Co., Ltd, Xiamen, Fujian, China). Optical density (OD) was measured on a VersaMax-BN03152 micro plate reader (Molecular Devices, Silicon Valley, CA, USA). ZHWY-2102 rotary shakers (Shanghai ZhiCheng Analyzing Instrument Manufactory Co., Ltd, Shanghai, China) were used for the fermentation processes.

Cell Lines and Reagents. Human chronic myelogenous leukemia K562 cells were provided by Li-Li Wang (Beijing Institute of Pharmacology and Toxicology, Beijing, China). Human cancer cells, acute promyelocytic leukemia HL-60, cervical cancer HeLa and gastric adenocarcinoma BGC-823, were provided by Wen-Xia Zhou (Beijing Institute of Pharmacology and Toxicology). Fetal bovine serum was purchased from Tianjin Hao Yang Biological Manufacture Co., Ltd (Tianjin, China). RPMI-1640 medium (lot no. 1403238) and MTT (lot no. 0793) were purchased from Gibco (Grant Island, NY, USA) and Amresco (Solon, OH, USA), respectively. Streptomycin (lot no. 071104) and penicillin (lot

no. X11303302) were purchased from North China Pharmaceutical Group Corporation (Beijing, China). 5-Fluorouracil (5-FU, lot no. 5402) was purchased from Aladdin Chemistry Co., Ltd (Shanghai, China).

Fungal Strains. The parent G59 strain was isolated from a soil sample collected at the tideland of Bohai Bay around Lüjühe in the Tanggu district of Tianjin, China, in September 2004.[2] The G59 strain was identified as *Penicillium purpurogenum* G59 by Liang-Dong Guo of the Institute of Microbiology of the Chinese Academy of Sciences, Beijing, China. This strain has been deposited at the China General Microbiological Culture Collection Center (CGMCCC) under the accession number CGMCC No. 9721. The fungal mutant AD-1-1 that was used as the producing strain in the current study is a bioactive mutant derived from the diethyl sulfate (DES) mutagenesis of *P. purpurogenum* G59. The mutant AD-1-1 strain was obtained by the treatment of fresh G59 spores with 0.5% (v/v) DES in 50% (v/v) DMSO at 4 °C for 1 day in our previous studies.[3] This mutant strain has been deposited at the CGMCCC under the accession number CGMCC No. 11656.

Fermentation and Extraction. Spore suspensions of the mutant AD-1-1 and parent G59 strains were prepared using fresh spores according to a previously reported procedure.[4] The spore density of the suspensions was adjusted to an OD value of 0.4 by monitoring the OD at 600 nm, which was measured on a VersaMax-BN03152 micro plate reader.

The producing fermentation of the mutant AD-1-1 was conducted in sixteen 500-mL Erlenmeyer flasks, each containing 80 g of rice. Distilled water (150 mL) was added to each flask, and the contents were soaked overnight before autoclaving at 121 °C for 30 min. After cooling to room temperature, an aliquot (200 μL) of the mutant AD-1-1 spore suspension was inoculated into each flask, and incubated at 28 °C for 45 days. The fermented material in each flask was extracted with 500 mL of ethyl acetate (EtOAc) under ultrasonic irradiation for 2 h to give an EtOAc solution. The EtOAc solutions obtained were combined, and the evaporation of the solution gave an EtOAc extract (40.1 g). This extract weakly inhibited K562 cells with an inhibition rate (IR%) of 21.7% at 100 μg/mL. Compounds **1–4** were isolated from this extract. The parent G59 strain was concurrently fermented and extracted in the same manner. Three 500-mL Erlenmeyer flasks were used to obtain an EtOAc extract (7 g). This extract did not exhibit any inhibitory effect on K562 cells (an IR% of 1.7% at 100 μg/mL). This extract was used as the negative control in the separation of the mutant AD-1-1 extract for tracking newly produced metabolites by the mutant. The EtOAc extracts of the mutant and parent strains were used in the HPLC-photo diode array detector (PDAD)-UV and HPLC-ESI-MS analyses to detect **1–4**.

Isolation of 1–4. The EtOAc extract (40 g) of the mutant AD-1-1 was fractionated by vacuum liquid chromatography on a silica gel column (silica gel, 300 g; bed, 7.5 × 20 cm) using a stepwise elution with dichloromethane (D)–methanol (M) to obtain fifteen fractions: **Fr-1** (2 g, eluted with D), **Fr-2** (1.7 g, eluted with D), **Fr-3** (140 mg, eluted with DM 99:1), **Fr-4** (30 mg, eluted with DM 98:2), **Fr-5** (70

mg, eluted with DM 98:2), **Fr-6** (350 mg, eluted with DM 96:4), **Fr-7** (1.3 g, eluted with DM 96:4), **Fr-8** (2.8 g, eluted with DM 96:4), **Fr-9** (3.5 g, eluted with DM 92:8), **Fr-10** (6.7 g, eluted with DM 90:10), **Fr-11** (2.1 g, eluted with DM 85:15), **Fr-12** (5.6 g, eluted with DM 85:15), **Fr-13** (10 g, eluted with DM 80:20), **Fr-14** (2.0 g, eluted with DM 70:30 → 50:50) and **Fr-15** (1.4 g, eluted with M). **Fr-1**, **Fr-2**, **Fr-4**, **Fr-5**, **Fr-6** and **Fr-9** inhibited K562 cells with IR% values of 42.9%, 22.1%, 39.0%, 54.1%, 21.5% and 37.5% at 100 μg/mL, respectively. HPLC-PDAD-UV analysis indicated, by examining the typical UV absorptions, that **1–4** were contained in **Fr-5**. Thus, the fraction **Fr-5** (70 mg) was further separated by preparative HPLC (column, Capcell Pak C_{18}, MG II, 20 × 250 mm, room temperature; mobile phase, 80% MeOH in H_2O; flow rate, 5.0 mL/min; detection wavelengths, 210 and 270 nm) to obtain **1** (4 mg, t_R = 16.9 min), **2** (4 mg, t_R = 19.2 min), **3** (3 mg, t_R = 17.8 min) and **4** (22 mg, t_R = 30.1 min).

HPLC-PDAD-UV and HPLC-ESI-MS Analysis. The EtOAc extracts of the mutant AD-1-1 and parent G59 strains were dissolved in MeOH to prepare sample solutions at 10 mg/mL for HPLC-PDAD-UV and HPLC-ESI-MS analyses. Compound **1** (in MeOH at 1 mg/mL) was used as the reference standard to determine retention times (t_R) of **1–4** according to their chromatographic behavior observed in the HPLC separation. HPLC-PDAD-UV analysis was performed on a Venusil MP C_{18} column (5 μm, 100 Å, 4.6 × 250 mm; Agela Technologies, Tianjin, China) using the Waters HPLC equipment described in the General Experimental Procedures. The sample and standard solutions were filtered using 0.22-μm pore membrane filters. Each 10 μL of the solutions was injected onto the column and the column was eluted using a linear gradient of MeOH-H_2O (20% MeOH at 0 min → 100% MeOH at 60 min → 100% MeOH at 90 min; flow rate, 0.8 mL/min). The acquired photodiode array data were processed using the Waters Empower™ software to obtain the targeted HPLC-PDAD-UV data. The retention times (t_R) of **1–4** were 44.02, 50.03, 49.17 and 58.55 min in the HPLC-PDAD-UV analysis, respectively. All of the compounds **1–4** were detected in the mutant AD-1-1 extract and not the parent G59 extract both by their t_R and UV spectra. HPLC-ESI-MS analysis was performed on a LC-MS equipment equipped with an Agilent 1100 HPLC system and an AB Sciex API 3000 LC-MS/MS system with AB Sciex Analyst 1.4 software (AB SCIEX, Framingham, USA). HPLC was run on the same Venusil MP C_{18} column (5 μm, 100 Å, 4.6 × 250 mm) under identical conditions to the HPLC-PDAD-UV analysis. The mass detector was set to scan a range of *m/z* 150 to 1,500 in both the positive and negative modes. The acquired data were processed using the Analyst 1.4 software to obtain the targeted HPLC-ESI-MS data. The *pseudo*-molecular ions of **1–4** appeared as peaks with t_R values of 41.5–42.1 min for **1**, 47.1–47.2 min for **2**, 46.61–46.63 min for **3** and 55.0–55.1 min for **4** in the HPLC-ESI-MS analysis. The retention time was slightly shorter than that observed in the HPLC-PDAD-UV analysis because of the shorter flow length from the outlet of the HPLC column to the inlet of the MS in the HPLC-ESI-MS system. Compounds **1–4** were also detected only in the mutant AD-1-1 extract, with no

evidence of these compounds in the parent G59 extract by selective ion monitoring (*m*/*z*: 327 $[M + Na]^+$ for **1**, 247 $[M + H]^+$ for **2**, 311 $[M + Cl]^-$ for **3** and 513 $[M + Na]^+$ for **4**) of the extracted ion chromatograms and the related MS data.

TDDFT Electronic CD (ECD) Calculations for 1, *ent*-1, 4 and *ent*-4. Conformational searches were performed employing the 'systematic' procedure implemented in Spartan'14,[5] using a MMFF (Merck molecular force field). All MMFF minima were re-optimized according to the DFT calculations at the B3LYP/6-31+G(d) level using the Gaussian 09 program.[6] The geometry was optimized starting from various initial conformations with vibrational frequency calculations confirming the presence of minima. TDDFT calculations were performed on the lowest-energy conformations (> 5% population) of each configuration using 20 excited states, using a polarizable continuum model (PCM) in MeOH. The ECD spectra were generated using the program SpecDis[7] by applying a Gaussian band shape with a 0.26-eV (for **1**) or 0.33-eV (for **4**) width from dipole-length rotational strengths. The dipole velocity forms yielded negligible differences. The spectra of the conformers for each of **1**, ***ent*-1**, **4** and ***ent*-4** were combined using Boltzmann weighting, with the lowest-energy conformations accounting for about 99% of the weights. The calculated spectrum was blue-shifted by 12 nm for **1**/***ent*-1** and 18 nm for **4**/***ent*-4** to facilitate comparison to the experimental data.

MTT Assay. The MTT assay was performed according to the previous procedure.[1-4] Exponentially growing K562, HL-60, HeLa and BGC-823 cells were treated with samples at 37 °C for 24 h. Assay was run in triplicate, and the OD value was determined at 570 nm on a VersaMax-BN03152 plate reader. The IR% was calculated using the mean value of the OD according to the formula: $IR\% = (OD_{control} - OD_{sample})/OD_{control} \times 100\%$. The EtOAc extracts, fractions and **1–4** in MeOH at 10.0 mg/mL, 5-FU (5-fluorouracil) in 20% (v/v) aqueous DMSO at 10.0 mg/mL and serial dilutions of the MeOH solution of **1** and **2** at 10.0 mg/mL were used in the MTT assay. 5-FU was used as the positive control. MeOH and 20% (v/v) aqueous DMSO solution were used as blank controls.

References

1. (a) C.-J. Wu, C.-W. Li and C.-B. Cui, *Mar. Drugs*, 2014, **12**, 1815; (b) M.-W. Xia, C.-B. Cui, C.-W. Li and C.-J. Wu, *Mar. Drugs*, 2014, **12**, 1545.
2. C.-K. Tian, C.-B. Cui and X.-X. Han, *J. Int. Pharm. Res.*, 2008, **35**, 401.
3. S.-M. Fang, C.-J. Wu, C.-W. Li and C.-B. Cui, *Mar. Drugs*, 2014, **12**, 1788.
4. (a) Y.-J. Chai, C.-B. Cui, C.-W. Li, C.-J. Wu, C.-K. Tian, and W. Hua, *Mar. Drugs*, 2012, **10**, 559; (b) S.-M. Fang, C.-B. Cui, C.-W. Li, C.-J. Wu, Z.-J. Zhang, L. Li, X.-J. Huang and W.-C. Ye, *Mar. Drugs*, 2012, **10**, 1266; (c) Y. Dong, C.-B. Cui, C.-W. Li, W. Hua, C.-J. Wu, T.-J. Zhu and Q.-Q. Gu, *Mar. Drugs*, 2014, **12**, 4326; (d) C.-J. Wu, L. Yi, C.-B. Cui, C.-W. Li, N. Wang and X. Han, *Mar. Drugs*, 2015, **13**, 2465; (e) M.-W. Xia, C.-B. Cui, C.-W. Li, J.-X. Peng and D.-H. Li, *Mar. Drugs*, 2015, **13**, 5219; (f) L. Yi, C.-B. Cui, C.-W. Li, J.-X. Peng and Q.-Q. Gu, *RSC Adv.*, 2016, **6**, 43975; (g) N. Wang, C.-B. Cui and C.-W. Li, *Arch. Pharm. Res.*, 2016, **39**, 762.
5. *Spartan'14*. Wavefunction Inc.: Irvine, CA, USA, 2013.
6. *Gaussian 09*, Revision A.01. Gaussian Inc.: Wallingford, CT, USA, 2009.

7. T. Bruhn, Y. Hemberger, A. Schaumlöffel, G. Bringmann, *SpecDis, Version 1.53*. University of Wuerzburg: Wuerzburg, Germany, 2011.

Physicochemical and Spectroscopic Data of Penicimutalidine (1)

Penicimutalidine (1): pale yellow needles (from MeOH), m.p. 104–105 °C, $[\alpha]_D^{25}$ +184.5 (*c* 0.21, MeOH). Positive ESIMS *m/z*: 322 $[M + NH_4]^+$, 327 $[M + Na]^+$, 359 $[M + CH_3OH + Na]^+$, 626 $[2M + NH_4]^+$, 631 $[2M + Na]^+$; negative ESIMS *m/z*: 303 $[M - H]^-$, 339 $[M + Cl]^-$, 366 $[M + CO(OH)_2]^-$, 607 $[2M - H]^-$, 643 $[2M + Cl]^-$. Positive HRESIMS *m/z*: measured 305.0668 $[M + H]^+$, calcd for $C_{15}H_{13}O_7$ 305.0661; measured 327.0479 $[M + Na]^+$, calcd for $C_{15}H_{12}O_7Na$ 327.0481. UV λ_{max} nm (log ε) in MeOH: 203.7 (3.77), 219.1 (3.91), 234.5 (4.00), 277.1 (3.71), 344.0 (3.25), and 364.0 (3.23). IR ν_{max} cm^{-1} (diamond ATR crystal): 3475, 3278 (OH), 3004 (Ar-H), 2955, 2854 (CH_3/CH), 1720 (ester CO), 1658 (conj. ester CO), 1630, 1616 1541 (Ar-ring), 1440, 1410, 1382 (CH_3), 1368, 1334, 1306, 1279, 1248, 1231, 1197, 1166, 1127, 1109, 1071, 1032, 839, 810, 775, 748, 721, 688, 653, 624, 528, 464. CD Δε (nm) in MeOH: −2.90 (200), −3.26 (205.5), 0 (216.0), +10.16 (238.5), 0 (249.5), −2.65 (shoulder peak, 256), −9.71 (284.5), 0 (308), +2.56 (340.5), +1.86 (371.5), 0 (434.5). 400 MHz ^1H and 100 MHz ^{13}C NMR data in acetone-d_6: Table S1.

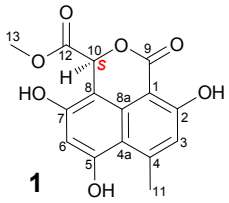

1

Table S1. 400 MHz ^1H and 100 MHz ^{13}C NMR data of **1** in acetone-d_6.

Position	δ_C [a]	δ_H [a] (*J* in Hz)	HMBC [c] (H → C)
1	98.0 s	—	—
2	163.9 s	—	—
3	117.6 d	6.68[b] q (0.8)	C-1, C-2, C-4a, C-12, C-9
4	148.7 s	—	—
4a	113.0 s	—	—
5	159.1 s	—	—
6	100.6 s	6.58 s	C-4, C-4a, C-5, C-7, C-8, C-10
7	155.2 s	—	—
8	98.3 s	—	—
8a	133.8 s	—	—
9	170.6 s	—	—
10	75.1 d	6.37 s	C-7, C-8, C-8a, C-9, C-11
11	25.3 q	2.82[b] 3H, d (0.8)	C-3, C-4, C-4a
12	170.3 s	—	—
13	52.9 q	3.64 3H, s	C-12
2-OH	—	11.73 s	C-1, C-2, C-3
5-OH	—	9.47 br s	C-4a, C-5, C-6
17-OH	—	9.38 br s	C-6, C-7, C-8

[a] δ_C and δ_H values were recorded using the solvent acetone-d_6 signals (δ_C 29.84 and δ_H 2.05) as references. The signal assignment was based on the results of ^1H–^1H COSY, HMQC, HMBC and NOESY experiments. [b] Cross peaks from the long-range allylic coupling between H-3 and H_3-11 were detected in ^1H–^1H COSY. [c] The numbers in each line of this column indicate the carbons that showed HMBC correlations with the proton in the corresponding line in HMBC experiments (optimized for the 8.3 of long-range J_{CH} value).

Physicochemical and Spectroscopic Data of Compounds 2–4

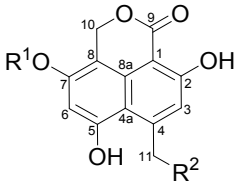

2: $R^1=R^2=H$
3: $R^1=CH_3$, $R^2=OH$

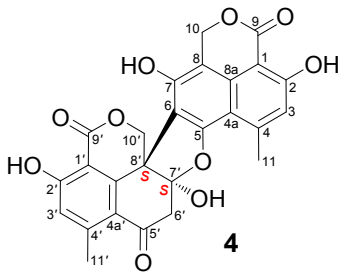

4

SF226 (2): yellow solid (from MeOH), m.p. 184–185 °C. Positive ESIMS *m/z*: 246 $[M]^+$, 285 $[M + K]^+$; negative ESIMS *m/z*: 245 $[M - H]^-$, 281 $[M + Cl]^-$, 291 $[M + CO_2H]^-$, 308 $[M + CO(OH)_2]^-$, 491 $[2M - H]^-$, 527 $[2M + Cl]^-$, 537 $[2M + CO_2H]^-$, 554 $[2M + CO(OH)_2]^-$. 400 MHz ^{1}H and 100 MHz ^{13}C NMR data in acetone-d_6: see Table 1 (in the main text).

Corymbiferan lactones A (3): yellow solid (from MeOH), m.p. 194–196 °C. Negative ESIMS *m/z*: 275 $[M - H]^-$, 311 $[M + Cl]^-$, 321 $[M + CO_2H]^-$, 338 $[M + CO(OH)_2]^-$, 551 $[2M - H]^-$, 587 $[2M + Cl]^-$, 597 $[2M + CO_2H]^-$, 614 $[2M + CO(OH)_2]^-$. 400 MHz ^{1}H and 100 MHz ^{13}C NMR data in DMSO-d_6 were identical to those in the literature (D. P. Overy and J. W. Blunt, *J. Nat. Prod.*, 2004, **67**, 1850).

Bacillosporin C (4): yellow solid (from MeOH), m.p. 184–185 °C, $[\alpha]_D^{25}$ +442.5 (*c* 0.20, MeOH). Positive ESIMS *m/z*: 513 $[M + Na]^+$; negative ESIMS *m/z*: 489 $[M - H]^-$, 979 $[2M - H]^-$. CD Δε (nm) in MeOH: −9.05 (200), −9.89 (205), –26.50 (216.0), 0 (226.5), +27.12 (246.5), +13.20 (shoulder peak, 262), +10.45 (shoulder peak, 270), 0 (283.3), –3.82 (292.5), 0 (308.5), +2.78 (323), +1.74 (shoulder peak, 351.5) 0 (385.5). 400 MHz ^{1}H and 100 MHz ^{13}C NMR data in acetone-d_6: see Table S2.

Table S2. 400 MHz ^{1}H and 100 MHz ^{13}C NMR data of **4** in acetone-d_6.[a]

Position	δ_H (*J* in Hz)	δ_C	Position	δ_H (*J* in Hz)	δ_C
1	—	97.8	1'	—	103.4
2	—	164.4	2'	—	164.7
3	6.76 q (1.0)	118.4	3'	6.91 q (0.8)	120.9
4	—	147.0	4'	—	150.2
4a	—	110.2	4a'	—	122.2
5	—	156.4	5'	—	193.4
6	—	114.7	6'	3.39 d (15.6)	49.7
				3.14 d (15.6)	
7	—	150.5	7'	—	112.4
8	—	112.4	8'	—	49.9
8a	—	133.2	8a'	—	145.0
9	—	170.54	9'	—	170.51
10	5.74 d (14.5)	67.5	10'	5.02 d (11.2)	74.1
	5.61 d (14.5)			4.77 d (11.2)	
11	2.78 d (1.0)	23.6	11'	2.59 d (0.8)	23.5
2-OH	11.75 s	—	2'-OH	11.99 s	—
7-OH	7.64 br s	—	7'-OH	8.65 br s	—

[a] δ_C and δ_H values were recorded using the solvent acetone-d_6 signals (δ_C 29.84 and δ_H 2.05) as references. The data listed in this table were identical to those of bacillosporin C in the literature (Z. Guo, *et al.*, *Magn. Reson. Chem.*, 2007, **45**, 439).

Figure S1. DFT-optimized structures for low-energy conformers of **1** and ***ent*-1** at the B3LYP/6-31+G(d) level using a polarizable continuum model (PCM) in MeOH (conformer population calculated using the Gibbs free energy and Boltzmann population at 298 K estimated thereof).

A: DFT-optimized structures for low-energy conformers of **1**

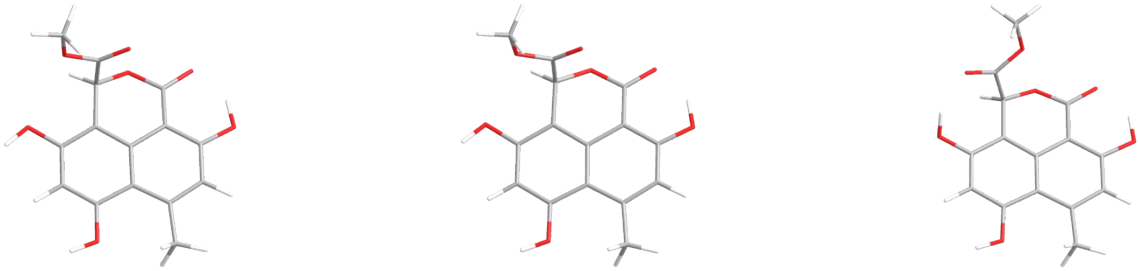

Conformer I (26.3%) Conformer II (26.6%) Conformer III (46.0%)

B: DFT-optimized structures for low-energy conformers of ***ent*-1**

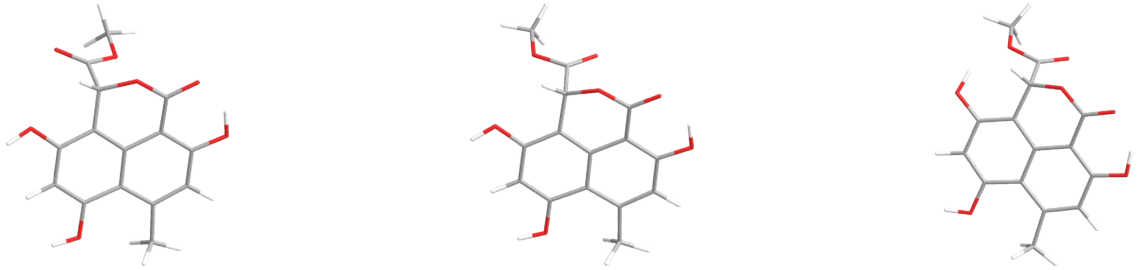

Conformer I (14.4%) Conformer II (50.9%) Conformer III (33.2%)

Figure S2. DFT-optimized structures for low-energy conformers of **4** & ***ent*-4** at the B3LYP/6-31+G(d) level using a polarizable continuum model (PCM) in MeOH (conformer population calculated using the Gibbs free energy and Boltzmann population at 298 K estimated thereof).

A: DFT-optimized structures for low-energy conformers of **4**

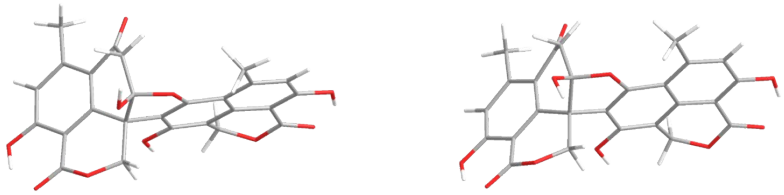

Conformer I (74.4%) Conformer II (25.5%)

B: DFT-optimized structures for low-energy conformers of ***ent*-4**

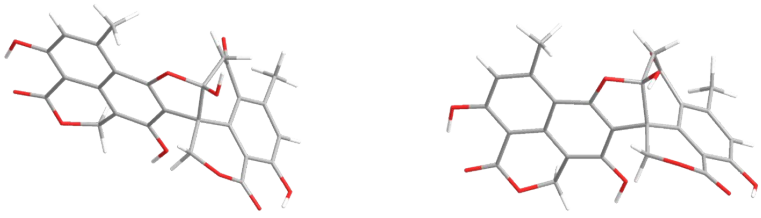

Conformer I (74.4%) Conformer II (25.5%)

Figure S3. HPLC-ESI-MS analysis of the EtOAC extracts of the mutant AD-1-1 and parent G59 strains to detect **1**–**4**.

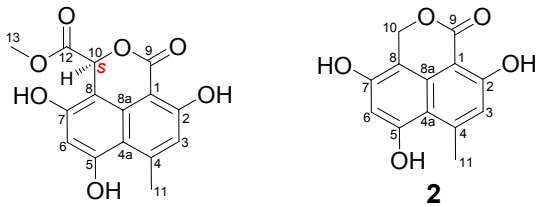

A: HPLC-positive ESI-MS analysis of the EtOAc extracts to detect **1**

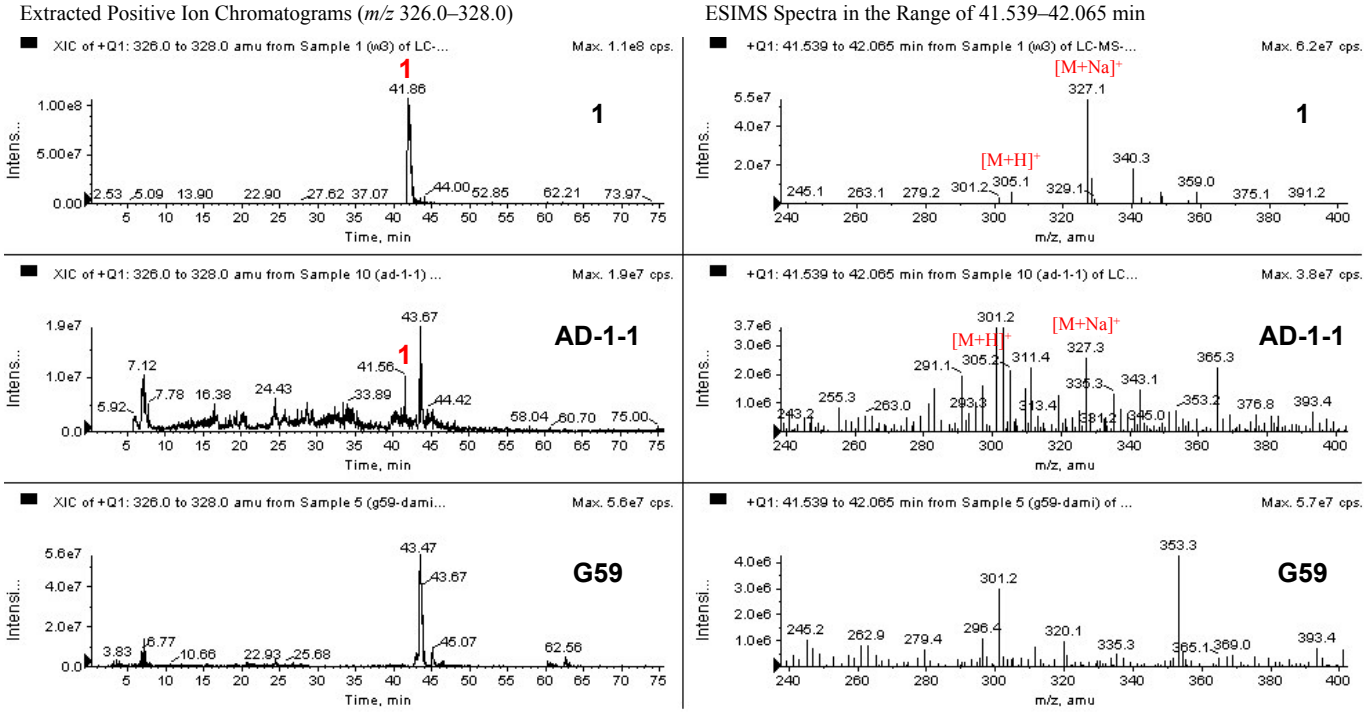

B: HPLC-positive ESI-MS analysis of the EtOAc extracts to detect **2**

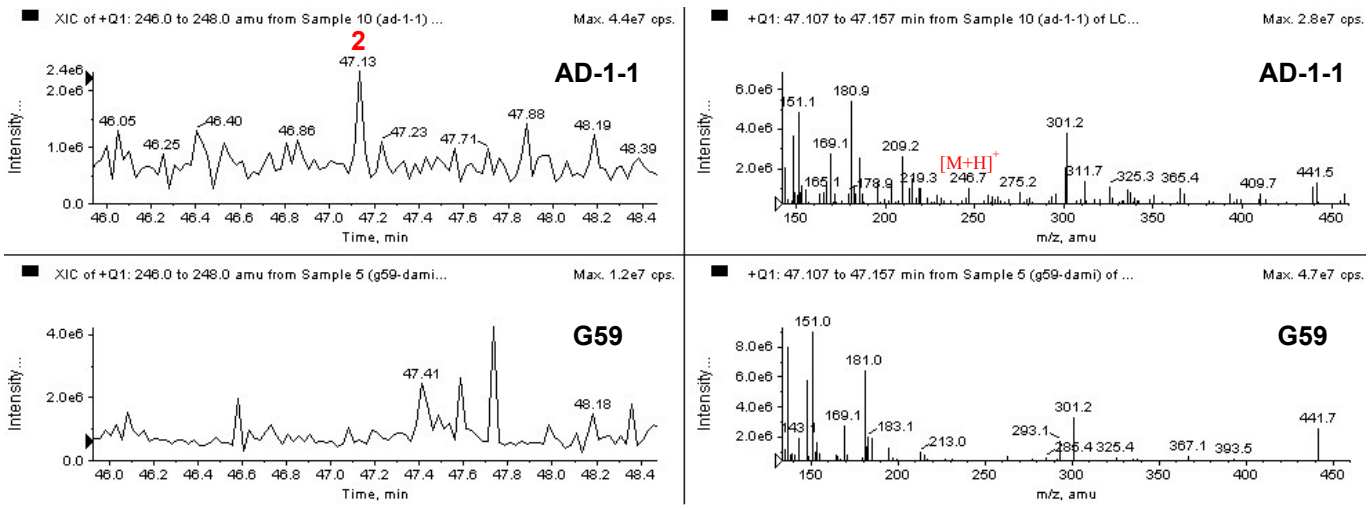

Figure S3. *Continued*.

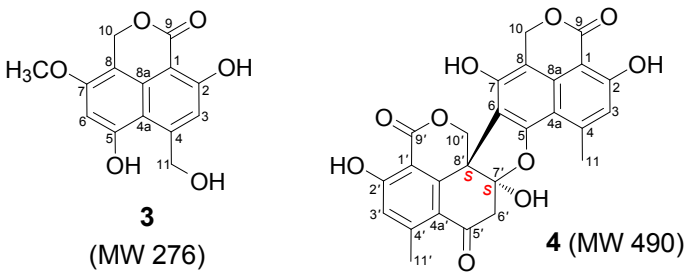

C: HPLC-negative ESI-MS analysis of the EtOAc extracts to detect **3**

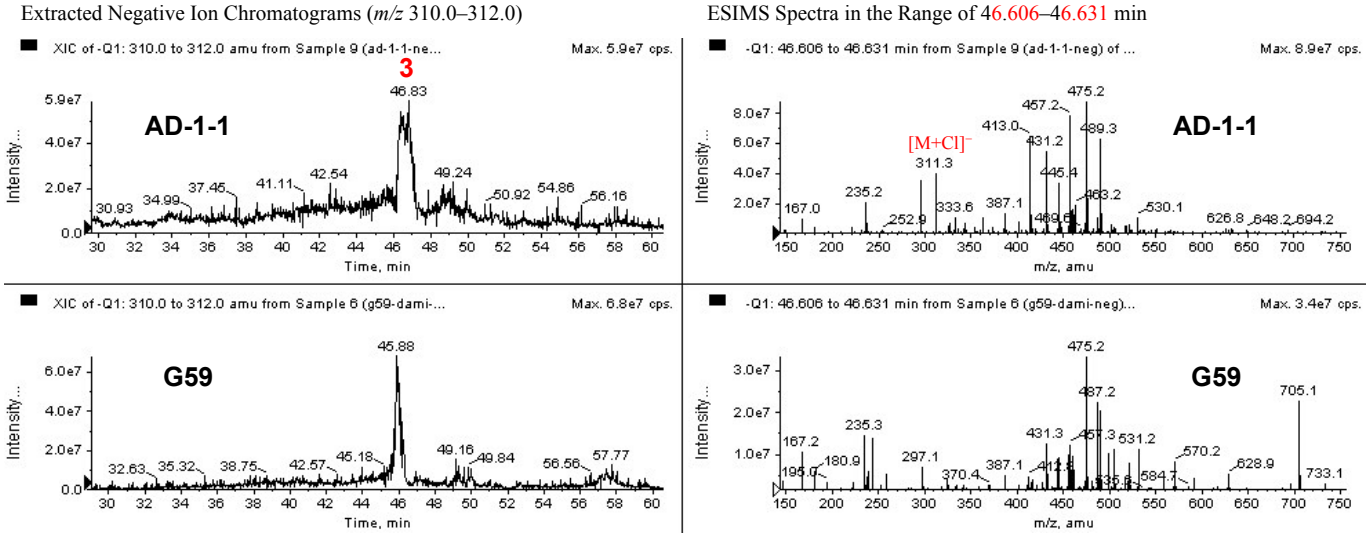

D: HPLC-positive ESI-MS analysis of the EtOAc extracts to detect **4**

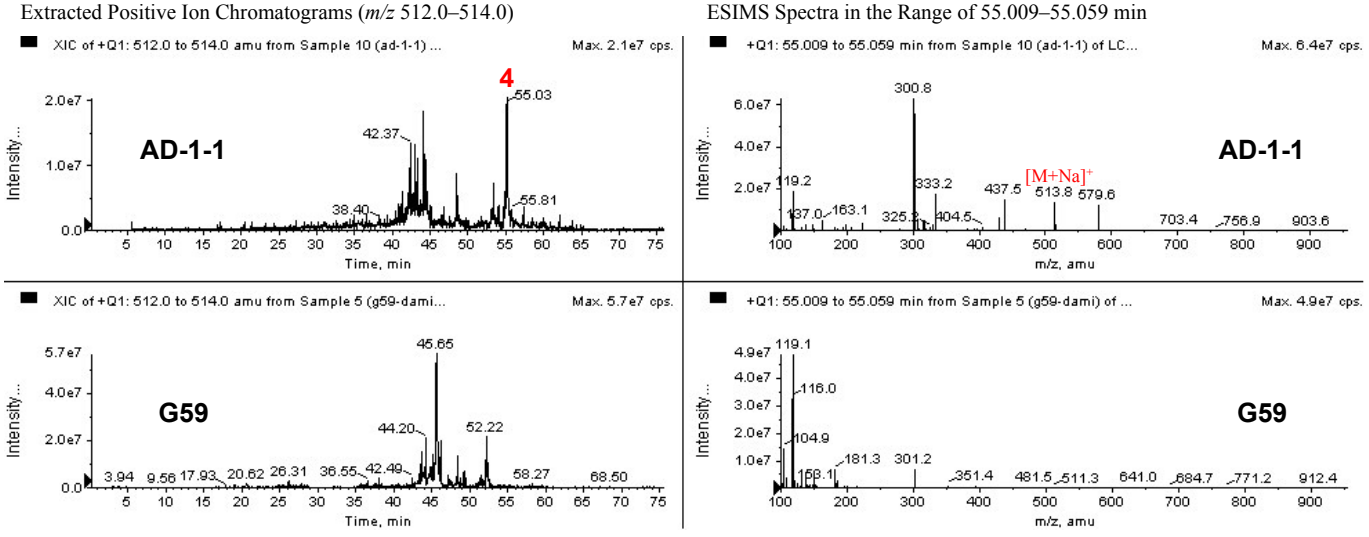

Figure S4. HPLC-UV analysis of the EtOAC extracts of the mutant AD-1-1 and parent G59 strains to detect **1–4**.

A: HPLC profiles detected at 210 and 270 nm

Conditions of HPLC: Venusil MP C_{18} column (5 μm, 100 Å, 4.6 × 250 mm), temperature, 25 °C; mobile phase, MeOH−H_2O in linear gradient (20% MeOH at 0 min → 100% MeOH at 60 min → 100% MeOH at 90 min); flow rate, 0.8 mL/min

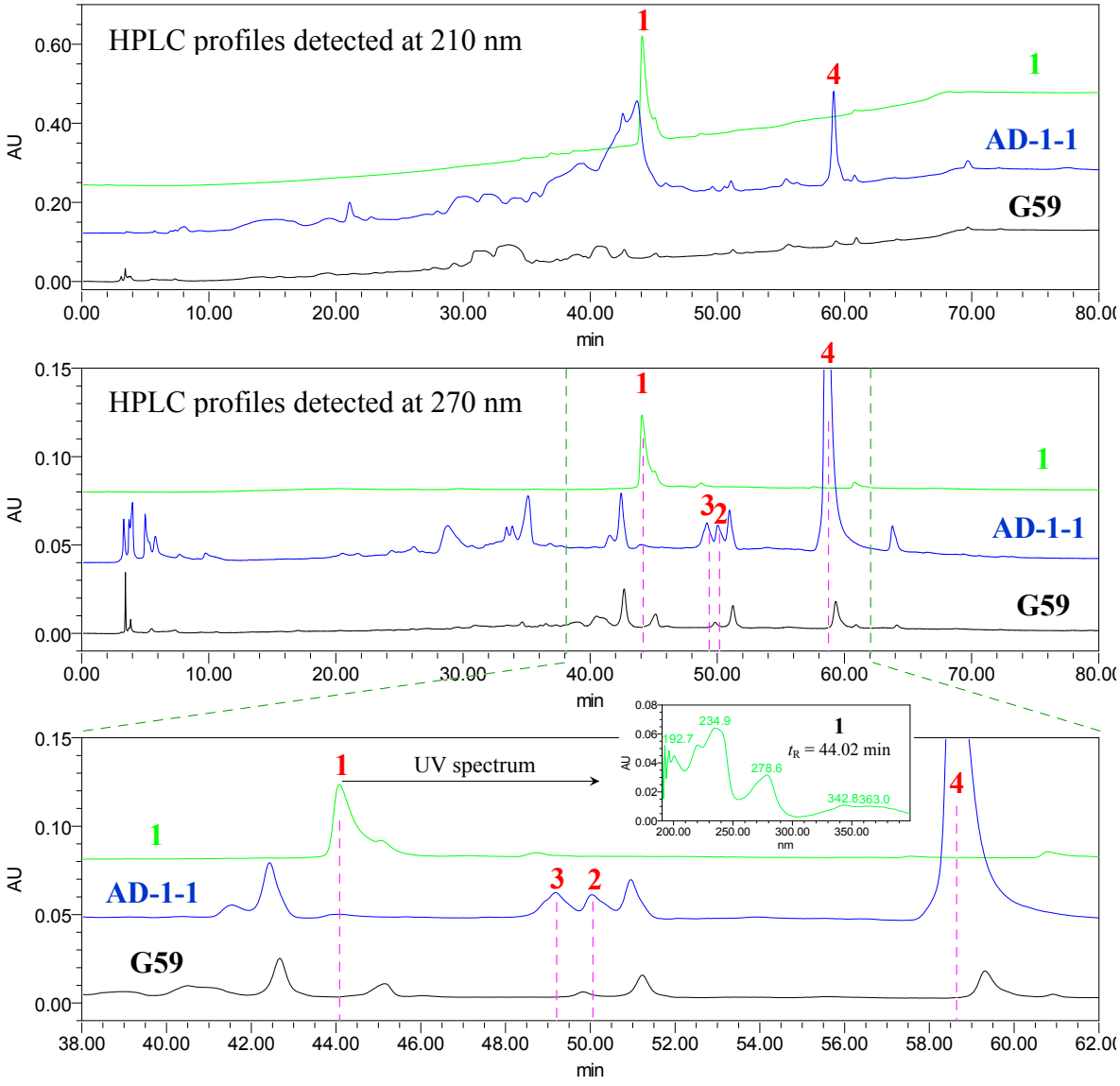

B: UV spectra at the retention times of **1–4**

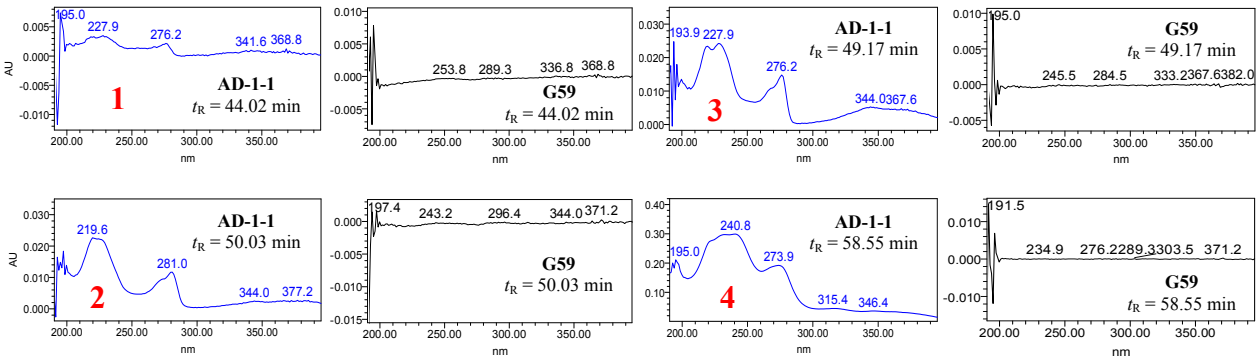

Figure S5. Positive (A) and negative (B) ESIMS spectra of **1.**

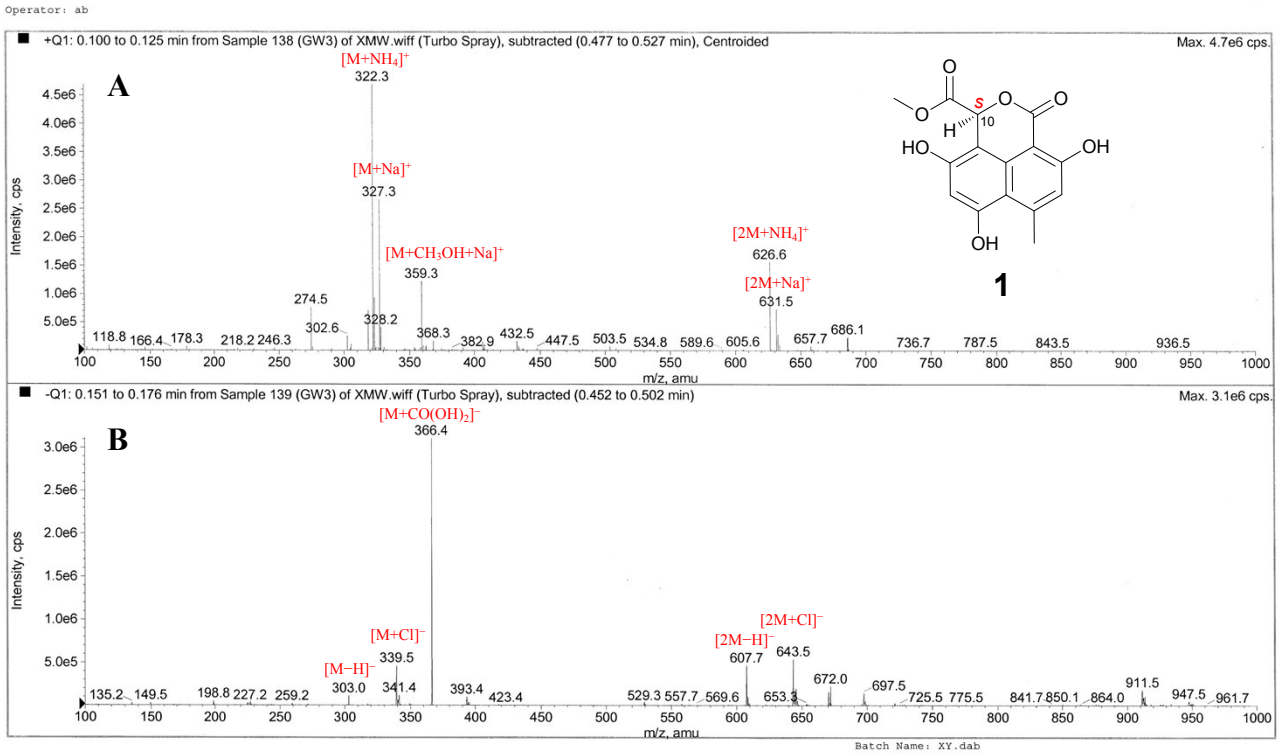

Figure S6. Positive HRESIMS spectrum of **1.**

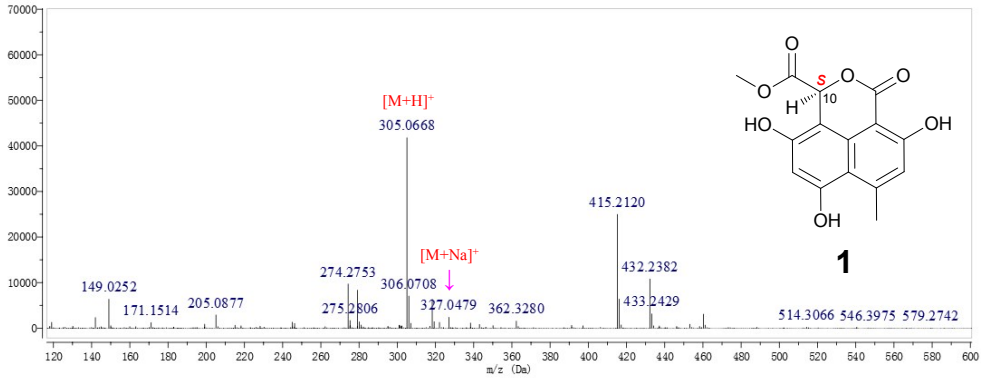

Figure S7. UV spectrum of **1** in MeOH**.**

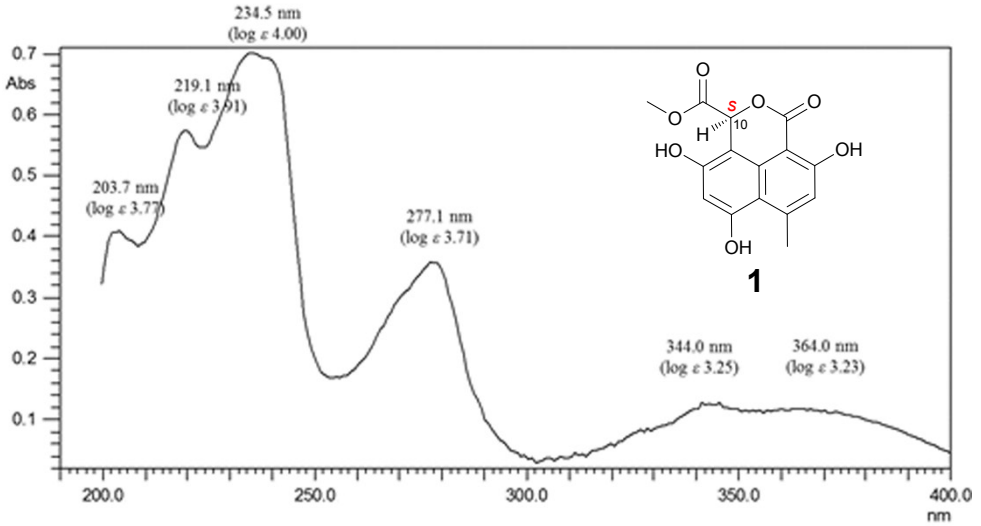

Figure S8. IR spectrum of **1** (measured on an ATR crystal).

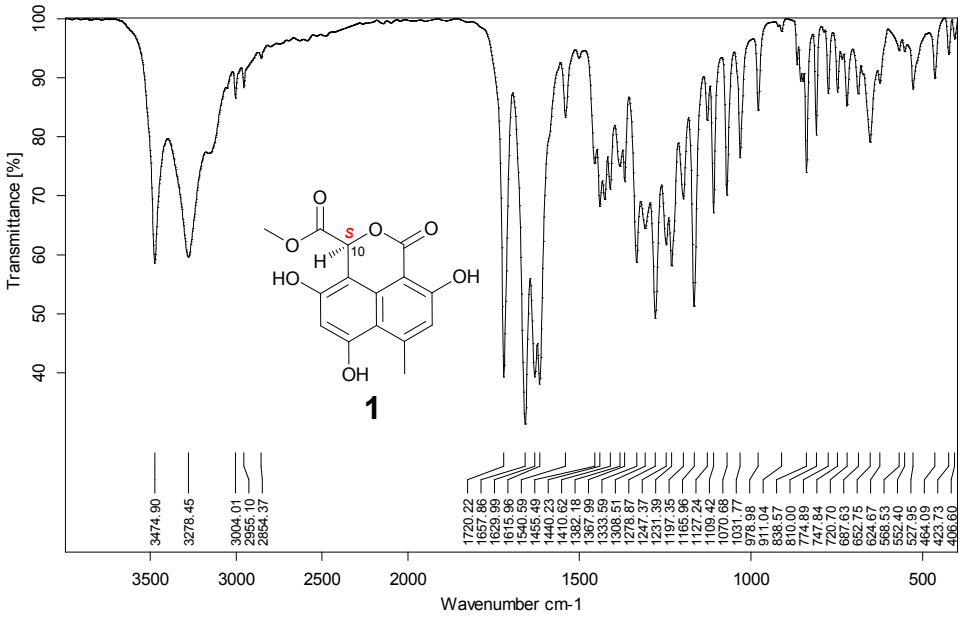

Figure S9. 400 MHz ^{1}H NMR spectrum of **1** in acetone-d_6.

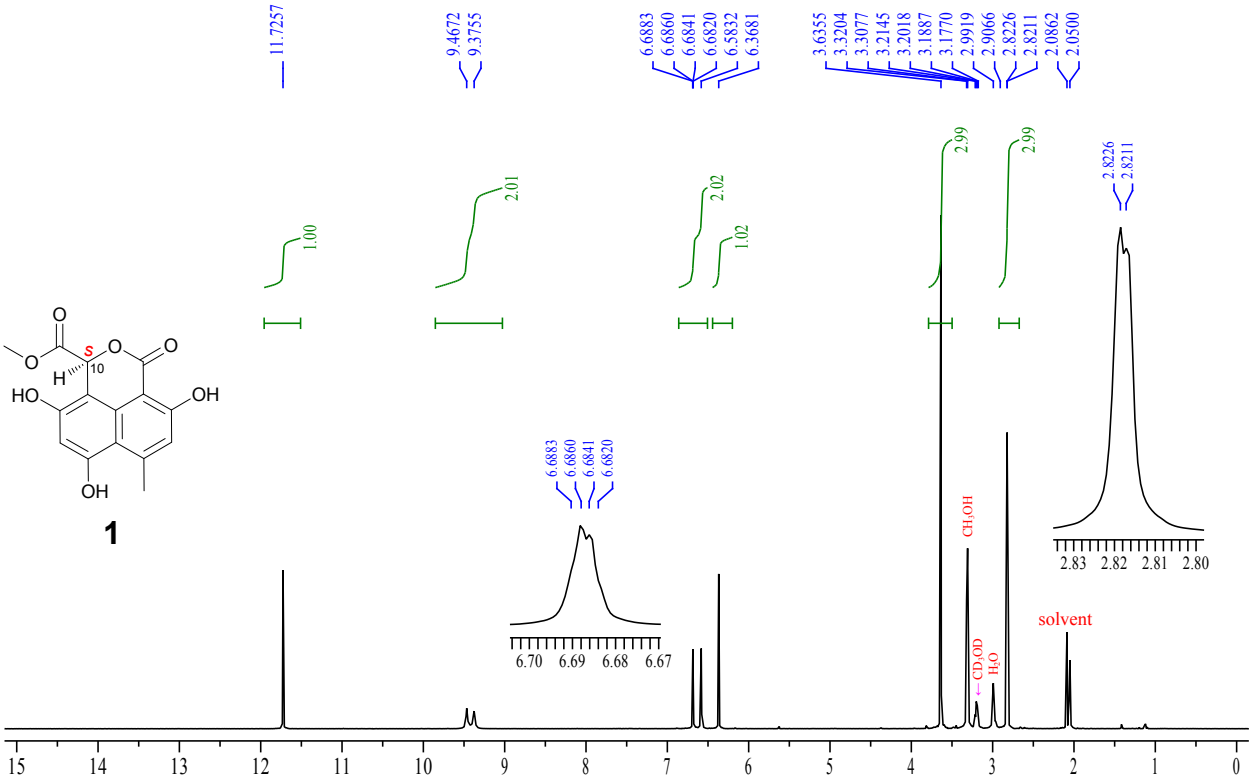

Figure S10. 100 MHz ^{13}C NMR spectrum of **1** in acetone-d_6.

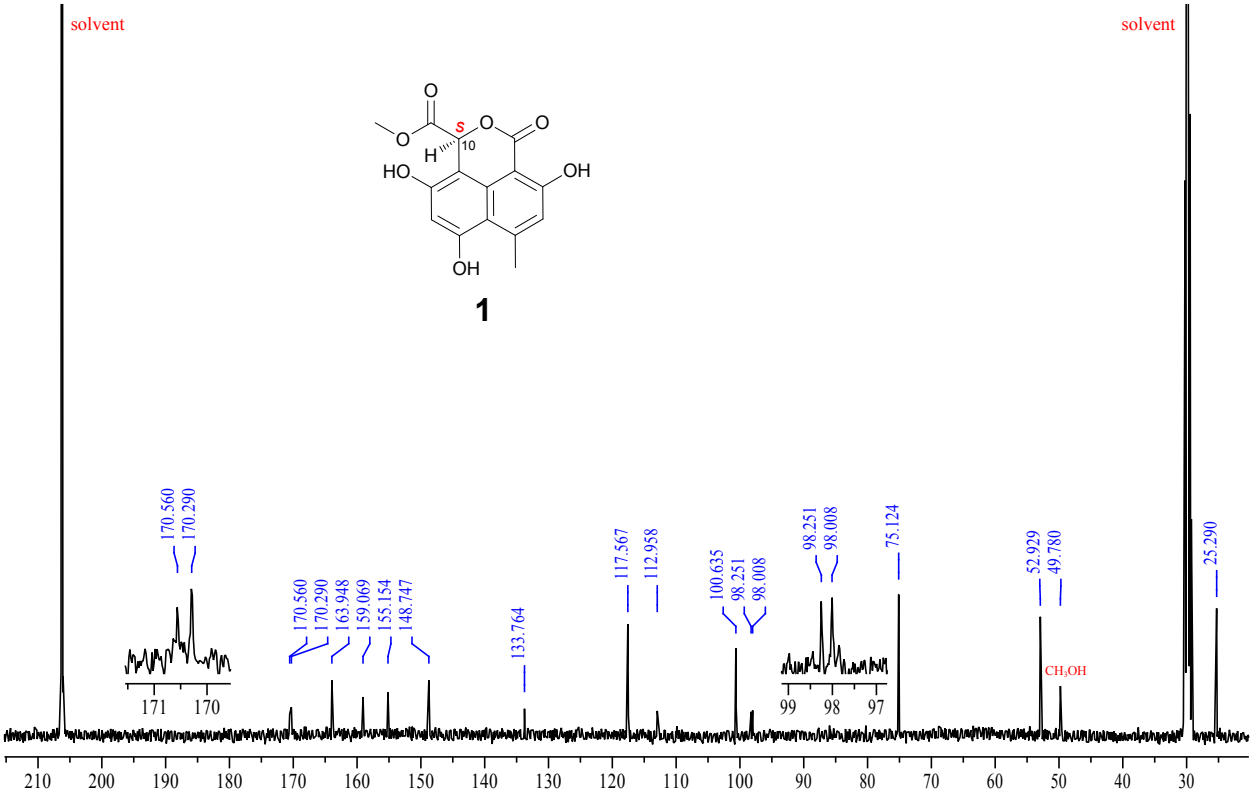

Figure S11. 400 MHz ^{1}H-^{1}H COSY spectrum of **1** in acetone-d_6.

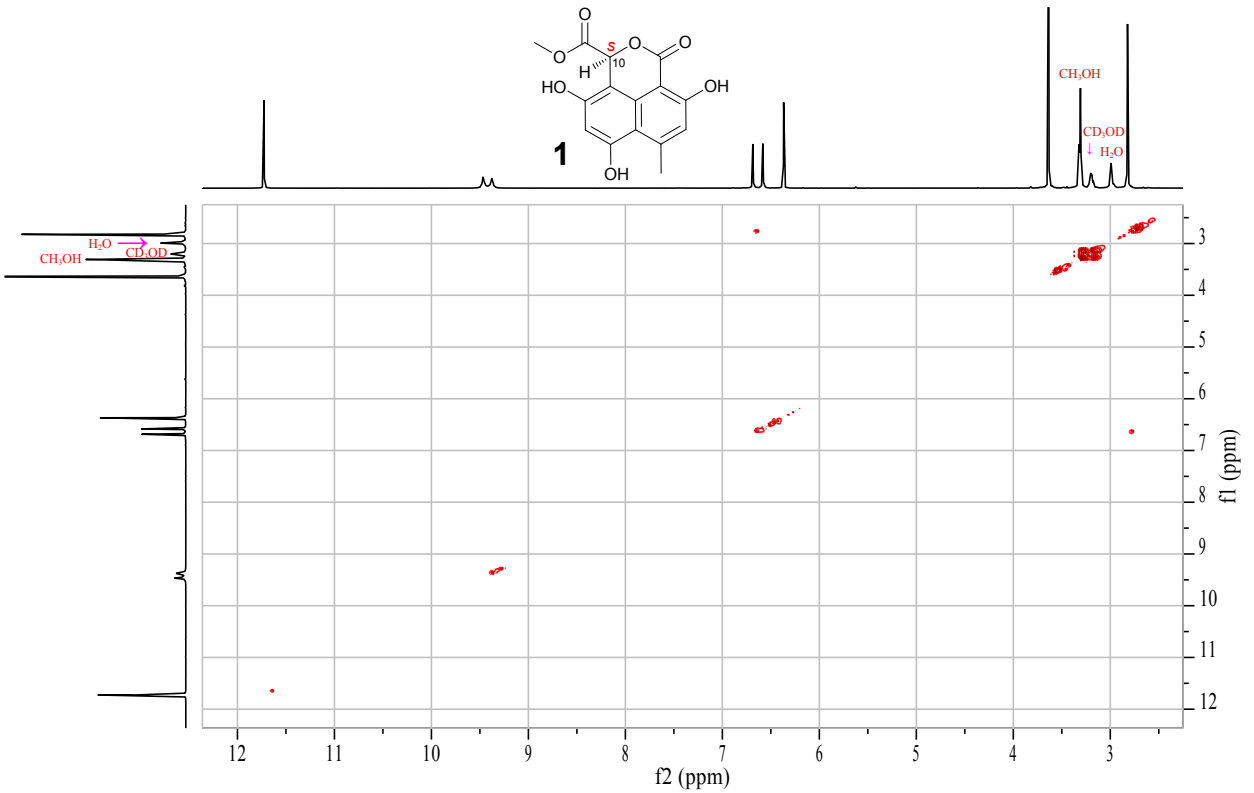

Figure S12. 400 MHz ^{1}H/100 MHz ^{13}C HMQC spectrum of **1** in acetone-d_6.

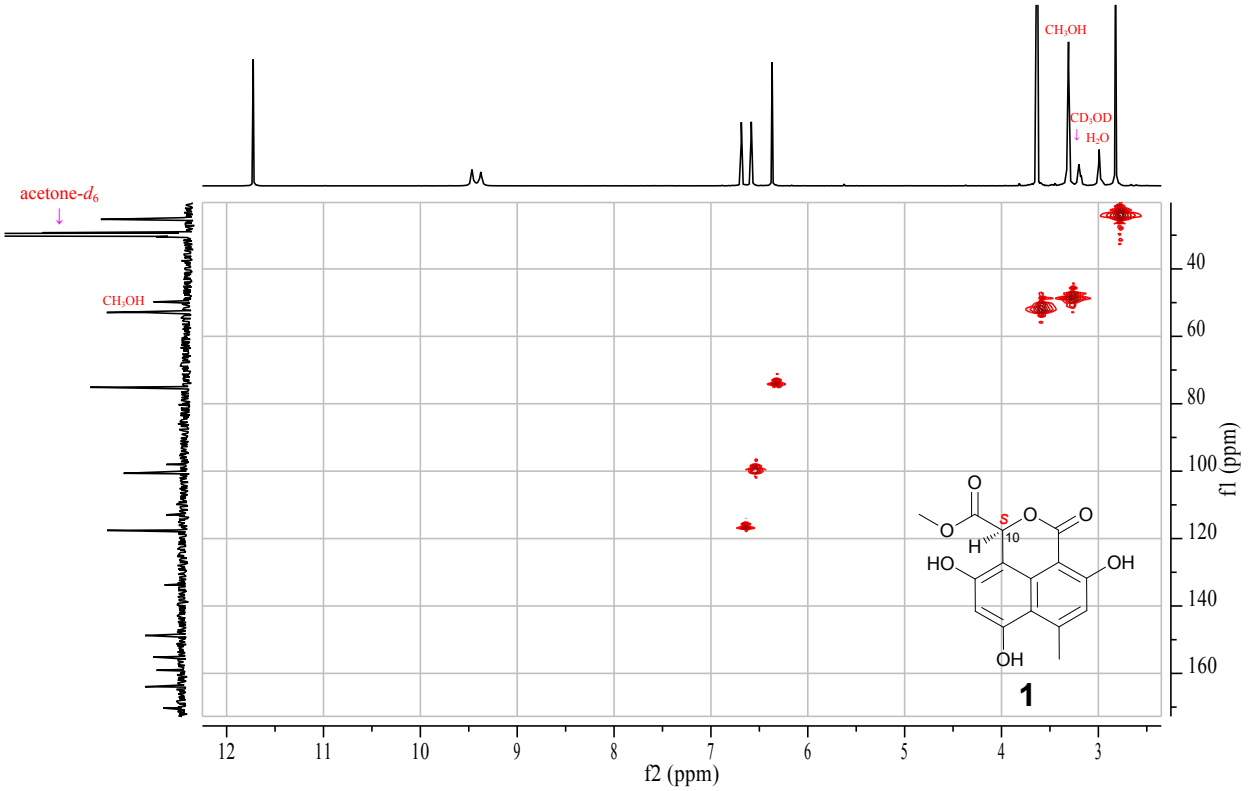

Figure S13. 400 MHz ^{1}H/100 MHz ^{13}C HMBC spectrum of **1** in acetone-d_6.

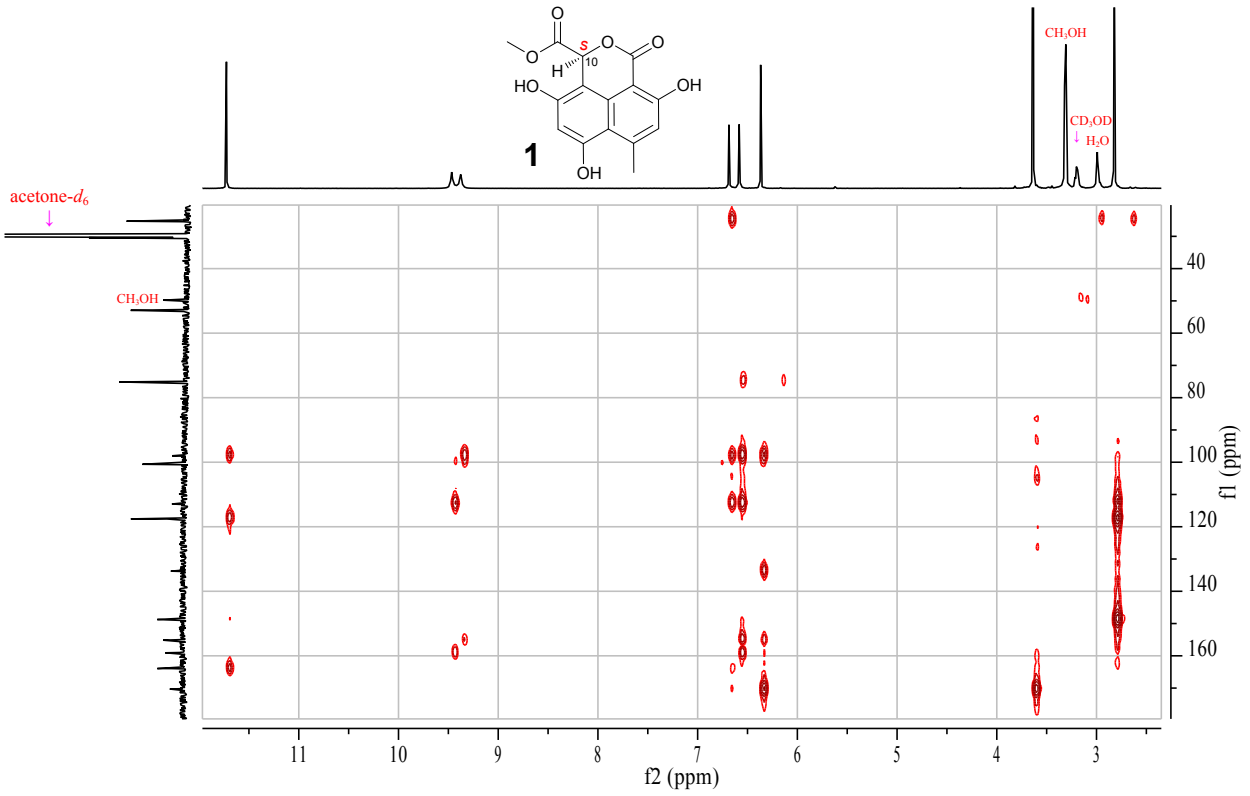

Figure S14. 400 MHz ^{1}H NMR spectrum of **4** in acetone-d_6.

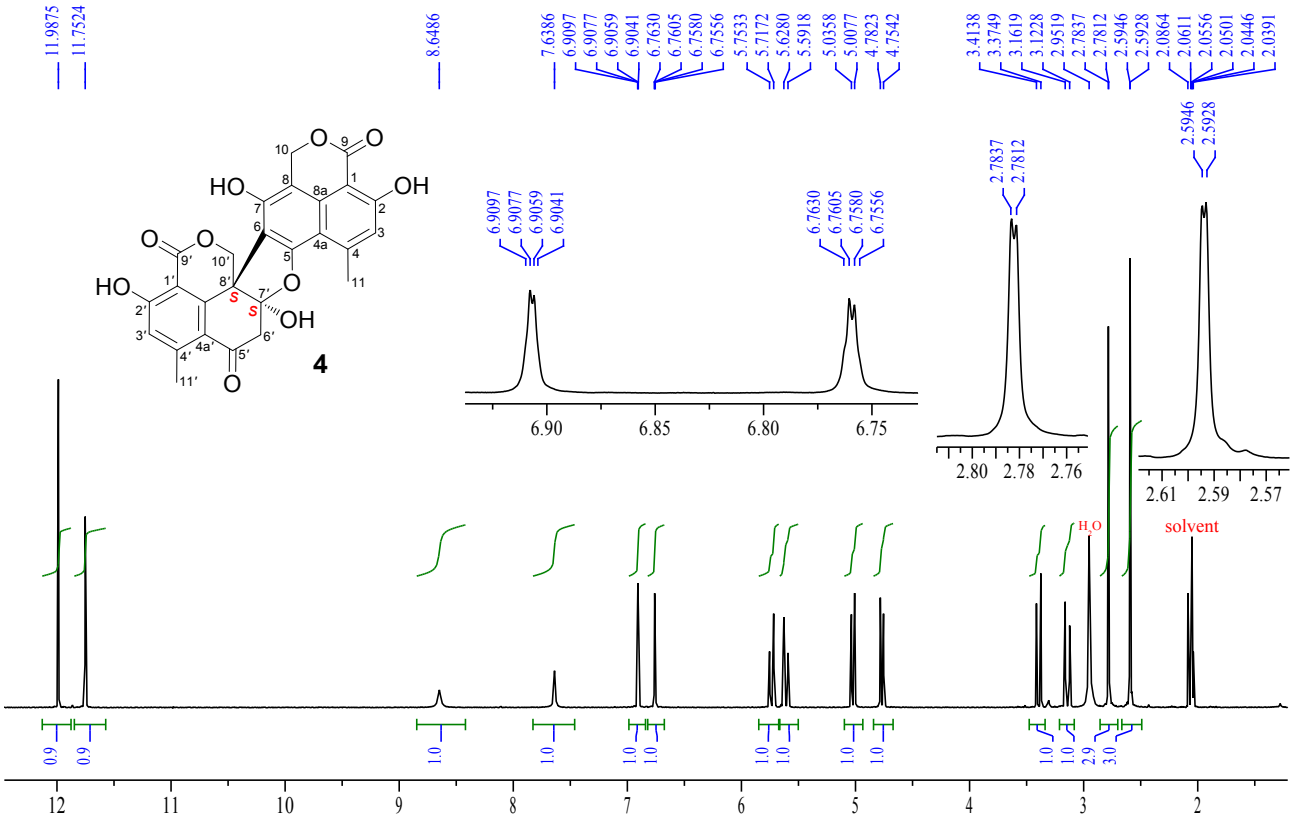

Figure S15. 100 MHz ^{13}C NMR spectrum of **4** in acetone-d_6.